Fourier Transform Rheometry on Carbon Black Filled Polybutadiene Compounds

Jean L. Leblanc

Universite P. & M. Curie (Paris 6), Polymer Rheology and Processing, 60 rue Auber, F-94408 Vitry-sur-Seine Cedex, France

Received 1 December 2003; accepted 26 March 2004
DOI 10.1002/app.21941
Published online in Wiley InterScience (www.interscience.wiley.com).

ABSTRACT: A series of high cis-1,4 polybutadiene compounds with various levels of N330 carbon black were prepared and tested using a Rubber Process Analyzer RPA® (Alpha Technologies), suitably modified for so-called Fourier transform rheometry. Strain sweep test protocols were used in order to capture strain and torque signals, that were consequently treated through Fourier transform calculations, using the appropriate proprietary software. Through strain sweep tests, the non-linear viscoelastic behavior was investigated, with significant odd-harmonics detected in the torque response, not only as the strain magnitude increases but also as the carbon black level increases. Differences in non-linear behavior, due to growing filler level are easily and clearly detected and the dependence upon strain of the relative third harmonic component is adequately modelled with simple four parameter models. Two such models were compared and found to give similar results, both offering two parameters to describe the strain sensitivity. First derivatives of the models allow a single number, i.e., the slope at a given strain, to be calculated as a "quantification" of the strain sensitivity, and hence of the non-linear character. Carbon black volume fraction appears then as the main compounding parameter influencing the non-linear viscoelastic response. © 2006 Wiley Periodicals, Inc. J Appl Polym Sci 100: 5102–5118, 2006

Key words: elastomers; fillers; polybutadiene; rheology; viscoelastic properties

INTRODUCTION

Fourier transform (FT) rheometry is a development of so-called dynamic (or harmonic) testing that allows both the linear and the nonlinear viscoelastic domains of polymer materials to be accurately investigated. Contrary to standard dynamic testing, for which strict proportionality between strain and strain is required for valid resolution of the (measured) complex modulus into its elastic and viscous components, this new technique suits particularly well complex polymer systems whose main characteristic is generally a strong nonlinear viscoelastic behavior. Any dynamic rheometer can conveniently be modified for FT testing to capture the full strain and torque signals generated when submitting samples to harmonic deformations at fixed frequency and temperature. Fourier transform calculation techniques are then applied to captured signals to resolve them in their main component and other harmonics, if any.

Filled rubber materials need special instruments for rheometrical testing, for instance the Rubber Process Analyzer RPA (Alpha Technologies). Such an instrument was modified for capturing strain an torque signals, through an appropriate software developed using LabView; details of the modification, as well as a description of the measuring technique, have been previously reported.[1] Through strain sweep tests, the nonlinear viscoelastic behavior of various gum elastomers was investigated and significant odd-harmonics were detected in the torque response.[2] It was demonstrated that the appropriate treatment of such harmonic torque components provides an easy quantification of the viscoelastic character, with a strong influence of the macromolecular structure, as expected.

Considering filled materials is a logical sequel of the works mentioned above, because complex polymer systems are known to exhibit a strong nonlinear viscoelastic character. Whatever their chemical nature, nearly all heterogeneous materials exhibit complicated responses when submitted to strain or to flow, but good engineering practices allow it to be somewhat controlled through pragmatic development. In the case of filled (rubber) materials, it is known while not fully understood that strong interactions between filler particles and polymer matrix play an important role in the flow properties of such materials. Following the pioneering work by Payne nearly 40 years ago, the significant reduction of elastic modulus with increasing strain amplitude of filled (vulcanized) elastomers, usually termed the Payne effect, has been

Correspondence to: J. L. Leblanc (jean.leblanc@ifoca.com).

TABLE I
Test Compounds

Compound coding:	BRC00	BRC10	BRC30	BRC50	BRC60
High *cis*-1,4 BR[a]	100	100	100	100	100
N330 carbon black	—	10	30	50	60
Zinc oxide	5	5	5	5	5
Oil	5	5	5	5	5
Stearic acid	3	3	3	3	3
TMQ[b]	2	2	2	2	2
IPPD[c]	1	1	1	1	1
Φ_{black}[d,f]	0	0.043	0.119	0.184	0.213
$\Phi_{fillers}$[e,f]	0.007	0.050	0.126	0.190	0.219

[a] Neocis-BR40 (Polimeri); 98% *cis*-1,4; M_w = 450,000 g/mol; MWD = 3.2.
[b] Trimethylquinoline, polymerized.
[c] Isopropylparaphenylenediamine.
[d] Carbon black volume fraction.
[e] (Carbon black + zinc oxide) volume fraction.
[f] Specific gravity data used in calculation (g/cm^3): R 0.90; N330 1.80; ZnO 5.57; Oil 0.92; St.Acid 0.98; TMQ 1.08; IPPD 1.17

investigated by a number of authors,[3,4] but the very mechanism for both reinforcement and nonlinearity remains a controversial issue. In contrast with the classical view that the Payne effect is due to the breakdown upon increasing strain of a secondary carbon black structure (the so-called carbon black network), assumed to exist in the compound in addition to the vulcanized rubber network, there are recent contributions that consider either stress-induced debonding of polymer chains from the filler surface[5] or release of trapped entanglements, i.e., temporary bonding of chains, from the filler surface.[6,7] Dynamic modulus decrease upon increasing strain amplitude has also been observed in unvulcanized systems,[7,8] but the associated loss of stress–strain proportionality (i.e., the basic condition for dynamic testing in linear viscoelastic condition) and the corresponding distortion of the harmonic signals were not directly considered, owing to instrument limitations. Fourier transform rheometry was essentially developed to fully document actual harmonic signals to provide insights into intrinsically nonlinear phenomena. For the present study, carbon-filled polybutadiene compounds were chosen with respect to the strong rubber–filler bonding that is known to be responsible for a number of their singular flow properties,[9] with the objectives to observe how extrinsic nonlinear viscoelasticity (as arising for large strain) combines with the intrinsic nonlinear character (i.e., due to the structure of the material) of complex polymer systems.

EXPERIMENTAL

Test materials

A series of filled polybutadiene compounds, as described in Table I, were prepared in a 1.4-L Banbury mixer through an upside-down mixing procedure and sheeted off on open mill. Dump temperature was between 100 and 110°C and mixing energy in the 1550 MJ/m^3 range for all compounds, which were stored at room temperature (23°C) under dark cover for 1 month before testing. Gum samples, hereafter coded BRN40, were cut from the bale, also stored at 23°C in darkness.

Test protocols for strain sweep experiments

With respect to its measuring principle, the RPA cavity must be loaded with a slight volume excess of test material. In agreement with ASTM 5289, the manufacturer recommends loading samples of around 5 g, i.e., 4.4 cm^3 for a standard filled rubber compound with a specific gravity of 1.14 g/cm^3. Using actual dimensions of the cavity[10], one can calculate its near exact volume by taking into account the grooves (2 × 24 small grooves of 1 × 1.57 × 9.6 mm; rounding of extremities is neglected) and by assuming that the central gap between upper and lower dies is 0.5 mm. A theoretical cavity volume of 3280 mm^3 is obtained. By considering a volume excess of 5%, optimized sample loadings are between around 3.25 g (zero black standard polybutadiene cpd; spec. grav. = 0.94 g/cm^3) and 3.90 g (60 phr carbon black filled BR cpd; spec. grav. = 1.13 g/cm^3). Samples for RPA testing were consequently prepared by die cutting 46-mm-diameter disks out of around 2-mm-thick sheets of materials. Each sample was weighed and, if necessary, adjusted to maintain its weight within the optimized loading ±0.2 g.

Strain sweep tests were performed with the RPA, according to protocols given in Table II. Each protocol describes strain sweep experiments through two subsequent runs separated by a resting period of 2 min. At least two samples of the same material were tested, using protocols named "Ssweep 1Hz A" and "Ssweep 1Hz B" such that, through inversion of the strain sequences (i.e., run 1 and run 2), sample fatigue effects would be detected, if any. At each strain sweep step, data acquisition (as described elsewhere[1]) was made to record 10,240 points at the rate of 512 pt/s. Twenty cycles were consequently recorded at each strain step, with the immediate requirement that the RPA was set to apply a sufficient number of cycles (i.e., 40 cycles; the so-called "stability" condition) for the steady harmonic regime to be reached. Data acquisition was activated as soon as the RPA test-monitoring screen had informed the operator that the set strain was reached and apparently stable.

With the protocols described in Table II, two subsequent strain sweep tests are performed within the limits of the instrument at the frequency considered, to capture signals up to the far nonlinear region, with evidence for strain sensitivity of the material, if any.

TABLE II
RPA Strain Sweep Test Protocols

Test protocol Ssweep_1Hz_A			Test protocol Ssweep_1Hz_B		
Strain sweep (run 1) Strain (°)	Dwell time	Strain sweep (run 2) Strain (°)	Strain sweep (run 1) Strain (°)	Dwell time	Strain sweep (run 2) Strain (°)
0.5	2 min, at rest	0.6	0.6	2 min, at rest	0.5
1.0		1.5	1.5		1.0
2.5		3.5	3.5		2.5
5.0		6.7	6.7		5.0
8.5		10.0	10.0		8.5
12.0		14.5	14.5		12.0
17.0		20.0	20.0		17.0
22.5		25.0	25.0		22.5
27.5		30.0	30.0		27.5
31.5		33.0	33.0		31.5

Note. RPA test conditions: Temp.(°C): as selected; Freq. (Hz): 1.
Sample conditioning: Preheating: 3 min, at rest; Fixing: 30 s; 1 Hz; 0.20°; Preheating: 2 min, at rest.

An experiment lasts some 23 min and two samples are tested using the two protocols in such a manner that the strain sequences of the successive runs are inverted. Should the tested material be sensitive to strain amplitude, differences are expected between runs 1 and 2, with the strain range documented by 20 experimental points. Such an experimental approach was designed to obtain the maximum number of data in the shortest test time (less than 1 h), while documenting in the meantime the test repeatability and the material homogeneity.

Fourier transform analysis

The modified RPA yields both strain and torque signals as recorded data files of actual harmonic strain and stress readings versus time. Conditions for optimal data capture were previously described,[2] which correspond to the following handling of the instrument : first the actual test conditions in terms of temperature, frequency, and strain angle are selected through built-in capabilities; then a sample is positioned on the lower die and the cavity is closed. The test is started and the data acquisition system is manually activated to record the selected number of data points (pt) with respect to the acquisition parameters used (i.e., 10,240 pt at 512 pt/s in this study).

A specific calculation program, written using the FT algorithm available in MathCad 8.0 (MathSoft, Inc.), was used to obtain the amplitude of the main stress and strain components (corresponding the test frequency) and the relative magnitudes (in percentages) of the odd-harmonic components.[16] The number of data points used, the frequency resolution (Hz), the acquisition time (s), and the sampling rate (point/s) are also provided. Figure 1 shows the averaged torque signal recorded when submitting a gum high *cis*-1,4 BR (i.e., NeoCis BR40, Polimeri) to 20° strain. As can be seen, the signal is harmonic but clearly distorted in comparison with a sinusoid of same amplitude. The displayed torque signal was averaged out of 20 recorded cycles (i.e., 10,240 data points) and the standard deviation drawn as a shaded area is barely visible, which demonstrates the excellent stability of the torque response. The single FT spectrum, obtained through calculation on the last 8192 points of the recorded torque (upper left in the figure), exhibits significant third and fifth harmonics, with further ones becoming very small. The results of the odd harmonic components analysis on both the torque and the strain signals are displayed in the inset table. The very low strain harmonic peaks (<0.55%) indicate the excellent quality of the applied signal, at least at this strain angle (20°).

RESULTS AND DISCUSSION

Harmonic strain signal quality

Ideal dynamic testing would require that a perfect sinusoidal deformation at controlled frequency and strain be applied on the test material. In the RPA, the (harmonic) strain of the material occurs by means of an oscillating wall, i.e., the lower die, through the monitored operation of a high-precision motor. A complex electronics continuously measures the oscillating angle and sends corrected "pulse" to the motor to obtain and maintain the set strain angle. Despite the high quality design and manufacturing of the instrument, there are, however, technical limits in accurately producing the harmonic mechanical motion, as with any other test devices. Fast Fourier transform of the

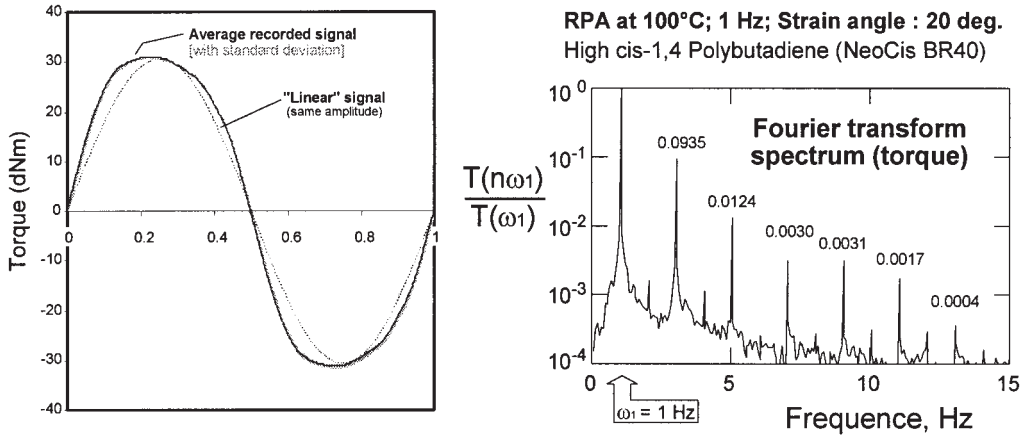

Fourier transform spectrum; odd harmonic components analysis

Nr pts	Freq.resol	**Main freq.**	3rd harm.	5th harm.	7th harm.	9th harm.	11th harm.	13th harm.	15th harm.
t_{aq}	Sampling pt/s	Main Torque a.u.	T(3/1),%	T(5/1), %	T(7/1), %	T(9/1), %	T(11/1), %	T(13/1), %	T(15/1), %
		Main Strain a.u.	S(3/1), %	S(5/1), %	S(7/1), %	S(9/1), %	S(11/1), %	S(13/1), %	S(15/1), %
8.192	0.063	**1**	3	5	7	9	11	13	15
7.998	512	**1541**	9.35	1.24	0.30	0.31	0.17	0.04	0.05
		911	0.55	0.27	0.14	0.08	0.05	0.01	0.00

Figure 1 Typical (averaged) torque traces as recorded when a gum polybutadiene sample is submitted to high strain; the Fourier transform spectrum exhibits accordingly significant harmonic contributions; the table gives the results of the automatic analysis of torque and strain signals.

strain (i.e., applied) signal allows this aspect to be documented, since no (significant) harmonics would be found in the strain signal if it were perfect.

A series of strain signals was thus captured by running the empty cavity of the RPA through strain sweep sequences either at 1.0- or at 0.5-Hz frequencies. Because a disturbing effect of cavity seals could be suspected, a few signal captures were performed without seals. Depending on the frequency, there are limits in maximum strain angle, for instance up to 33° (≈461%) at 1.0 Hz and some 65 ° (≈908%) at 0.5 Hz. No significant torque signal was of course obtained. For each test condition, 10,240 points were acquired and the last 8192nd ones ($=2^{13}$) were used to extract the Fourier transform spectra of the harmonic motion of the lower die. As expected, a linear relationship was observed between the set strain angle and the main strain component (in arbitrary units) revealed by FT analysis (Fig. 2). No influence of the seals and/or the frequency is noted. Linear regression yields a straight line of slope 45.56, which passes through zero. In terms of strain crest signal, the maximum oscillation angle of the lower die can therefore be considered nearly perfect.

FT analysis reveals, however, relatively significant (i.e., larger than noise) odd harmonics components, with obviously the 3rd harmonic the larger one. As shown in Figure 3, the relative 3rd harmonic component of strain signal decreases as strain amplitude increases, whatever the test conditions, i.e., with or without seals, and whatever the frequency. $S(3/1)$ passes below 1% of the main component when the strain angle is higher than 1.3–1.5°. Data obtained in all conditions superimpose well and a simple three-parameter hyperbolic decay equation was found adequate to model the observed effect, i.e.,

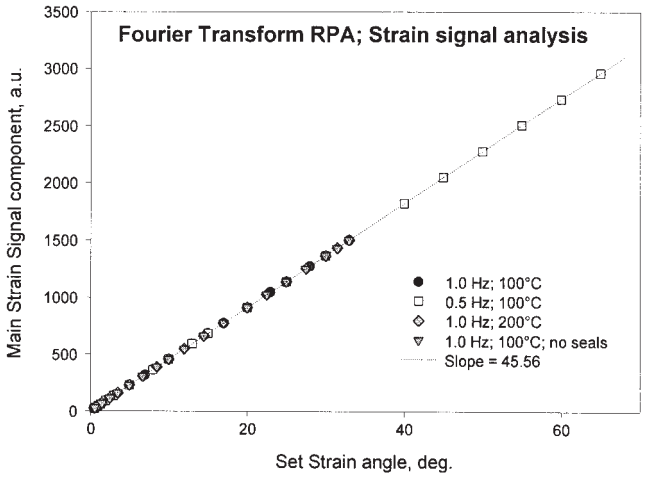

Figure 2 Applied strain angle quality, as demonstrated through the main strain signal component from Fourier Transform of recorded strain signal.

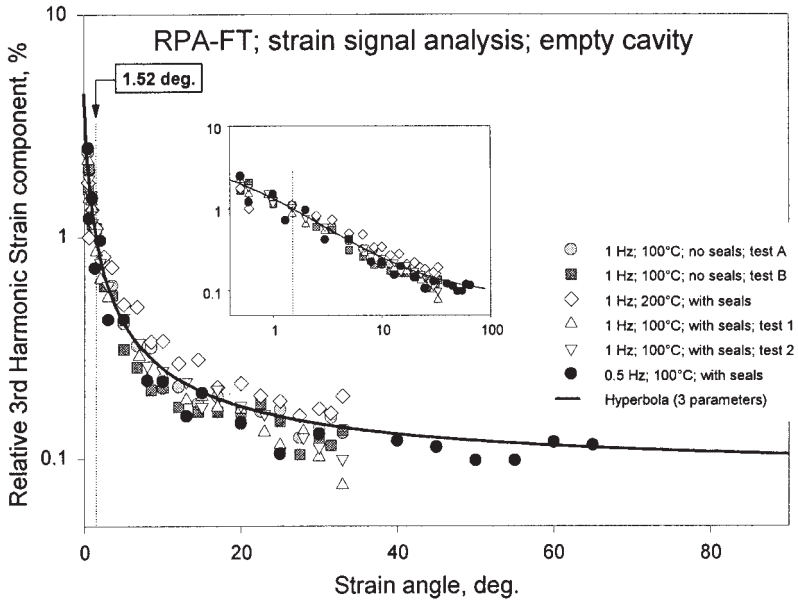

Figure 3 Analyzing strain signal quality through Fourier transform; strain signals recorded under various conditions with an empty cavity, with seals or without seals.

$$S(3/1) = a + \frac{bc}{c + \gamma} \quad (1)$$

where γ is the strain angle; a, b, and c fit parameters. The curve in Figure 3 was drawn with $a = 0.086$, $b = 4.31$, and $c = 0.408$ ($r^2 = 0.94$). The (hypothetical) zero strain component equal to 4.40%, which can be calculated using these parameters, has obviously no physical meaning, but demonstrates only that the lower the strain angle the poorer the quality of the applied strain signal. Equation (1) allows for calculating that, for the 3rd relative harmonic strain component to be below 1% of the main signal component, the strain angle must be higher than 1.52° (i.e., >21.2% deformation).

In developing an experimental set up for FT rheometry, with a commercial cone-and-plate rheometer (ARES; Rheometric Scientific), Wilhelm[11] found a slight nonlinear contribution from the instrument in the 10^{-3} to 10^{-4} range, relative to the response at the excitation frequency. In another publication[12], shear geometry, either cone-and-plate or parallel plates, was reported to affect the degree of nonlinear behavior as characterized by the $T(3\omega_1)/T(\omega_1)$ ratio. Similar geometrical effects are expected with the RPA, likely enhanced because measurements are made in a closed cavity in which the material is maintained under pressure. Since our approach consists of simultaneously analyzing the strain (input) and the torque (output) signals by Fourier transform, we have the capability to probe the quality of the strain signal when the test cavity is fully loaded. Figure 4 shows, for instance, how the $S(3\omega_1)/S(\omega_1)$ ratio varies with strain angle when performing strain sweep tests on our series of filled polybutadiene compounds. As can be seen, loading the cavity significantly increases the relative 3rd harmonic with respect to the $S(3/1)$ curve obtained when the cavity is empty. In addition, the actual stiffness of the material, imparted by the carbon black level, has a slight but significant effect, i.e., at equal strain angle, the higher the filler loading, the higher magnitude of the 3rd harmonic, as clearly shown in the insert where magnification was obtained by using logarithmic scales. The arrows indicate the strain angle for $S(3/1) = 1\%$, which moves to the right as carbon black level increases. Through local power law fitting, the strain angle values for $S(3/1) = 1\%$ are easily obtained, i.e., 4.91 ° (BRC10), 6.41 ° (BRC30), 7.82 ° (BRC50), and 9.94 ° (BRC60). It is worth emphasizing that, while the strain signal quality deteriorates somewhat when the test cavity is full, its quality nevertheless improves as the applied deformation increases.

Main torque component

Main torque components $T(\omega_1)$ are given in Appendixes I and II. Results obtained on two samples of the same test material superimpose well, which demonstrates their excellent homogeneity. Figure 5 shows how $T(\omega_1)$ varies with the set strain γ for all compounds. Strong nonlinearity is observed and the gum polybutadiene exhibits a significantly different behavior. In the low strain region, some curves seem to reduce to straight lines that would correspond to a linear behavior, i.e., $T(\omega_1)$ directly proportional to γ.

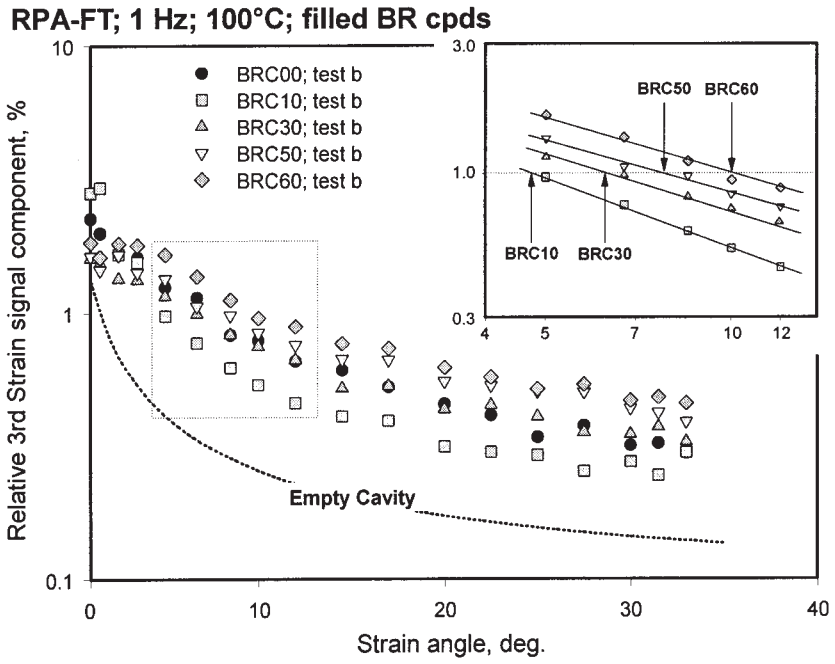

Figure 4 Analyzing strain signal quality through Fourier transform when the test cavity is loaded; compounds with different filler loadings were used.

Let us consider the curve obtained with the gum polybutadiene (Fig. 6). The ratio $T(\omega_1)/\gamma$ has obviously the meaning of a modulus and yields the most familiar picture of a plateau region at low strain, then a typical strain dependence (upper right inset). Note that with respect to the data acquisition conditions used for Fourier transform calculation, the following equality holds: G^* (kPa) = 12.335 × $T(\omega_1)/\gamma$ (with $T(\omega_1)$ in arbitrary units and γ in percentages). Such behavior is adequately modeled with the following equation, in which the reader will recognize the mathematical form of the so-called Cross equation for the shear viscosity function,

$$\frac{T(\omega_1)}{\gamma} = \left[\frac{T(\omega_1)}{\gamma}\right]_0 \times \left[\frac{1}{1 + (A\gamma)^B}\right], \qquad (2)$$

where $\left[\frac{T(\omega_1)}{\gamma}\right]_0$ is the modulus in the linear region, A is the reverse of a critical strain marking the limit be-

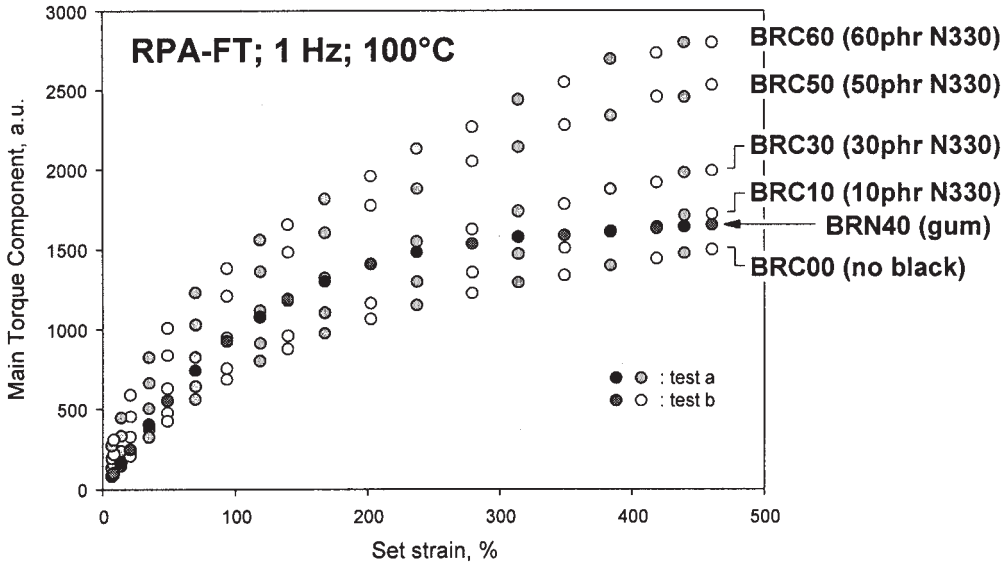

Figure 5 Main torque component $T(\omega_1)$ versus strain for filled BR compounds; data on gum BR are shown for comparison.

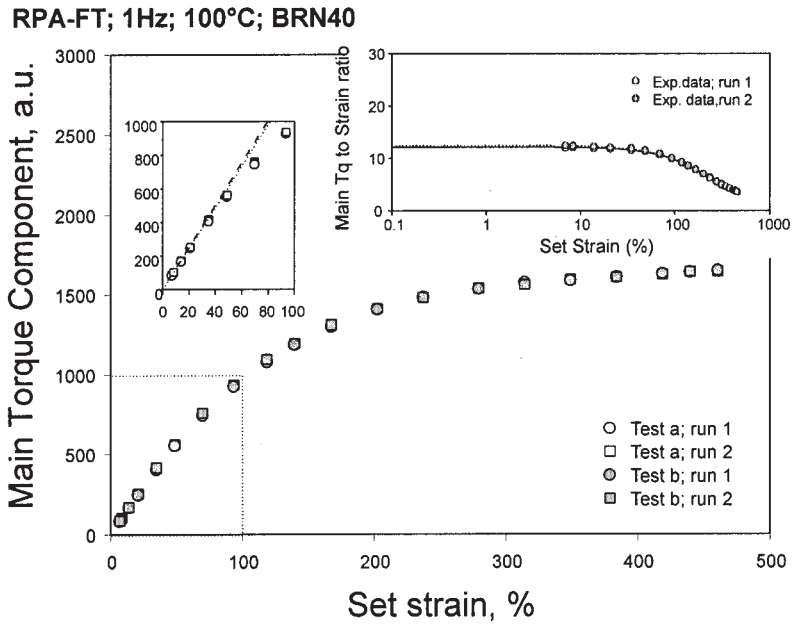

Figure 6 Main torque component when testing gum NeoCis BR40 sample (BRN40); deriving the linear modulus through modeling of $T(3/1)$ to strain ratio.

tween the linear and nonlinear regions, and B is a parameter describing the strain sensitivity of the material. The so-derived linear modulus is obviously the initial slope of the $T(\omega_1)$ versus γ, as illustrated in the upper left inset in Figure 6. No difference is seen between data gathered through runs 1 and 2, thus demonstrating that the gum material is not sensitive to strain history or that any memory effect is conveniently damped down during the resting period (2 min) between the two runs.

Table III gives the fit parameters of Eq. (2) for all the materials tested. Figure 7 shows data with the 60-phr carbon black filled compound. Here the picture is notably different, as no linear behavior is observed within the experimental window (i.e., 6.98 to 461%; 0.5 to 33°). In addition, runs 1 and 2 are significantly different, which suggests that the (rubber–filler) morphology has somewhat been altered when straining the material up to 31–33°. When expressed in terms of modulus, i.e., $T(\omega_1)/\gamma$ the strain history effect is even more appearing and the curvature in the low strain region suggests to fit the data with Eq. (2). The fit curves, drawn in the lower right inset, show that (largely) extrapolated linear modulus data can be obtained, which correspond indeed to the initial slopes of $T(\omega_1)$ versus γ curves.

TABLE III
Main Torque Component $T(\omega_1)$ versus Strain γ; Fitting Parameters for Eq. (2)

Material, run	$\left[\frac{T(\omega_1)}{\gamma}\right]_0$	A	B	r^2
BRN40, run1	12.15	4.00×10^{-3}	1.49	0.9994
BRN40, run2	12.49	4.16×10^{-3}	1.47	0.9996
BRC00, run1	10.17	4.59×10^{-3}	1.07	1.0000
BRC00, run2	10.23	4.66×10^{-3}	1.06	0.9994
BRC10, run1	12.04	5.12×10^{-3}	0.99	0.9978
BRC10, run2	14.00	6.20×10^{-3}	1.00	0.9993
BRC30, run1	19.27	9.33×10^{-3}	0.86	0.9991
BRC30, run2	17.50	8.24×10^{-3}	0.85	0.9995
BRC50, run1	34.07	2.11×10^{-2}	0.73	0.9996
BRC50, run2	29.86	1.87×10^{-2}	0.70	0.9995
BRC60, run1	53.10	4.16×10^{-2}	0.69	0.9996
BRC60, run2	43.22	4.14×10^{-2}	0.61	0.9994

The compounding variable in the work reported here is the filler level that can be expressed in term of volume fraction Φ_{black}. Figure 8 shows how the three parameters of Eq. (2) vary with Φ_{black}. As shown in the upper right plot, the linear modulus $\left[\frac{T(\omega_1)}{\gamma}\right]_0$ increases strongly with the carbon black content, in a manner markedly differing from the well-known Guth–Gold model[13,14], i.e., $G_{cpd}=G_0(1+2.5\times\Phi_{black} +14.1\times \Phi_{black^2})$. For instance using $G_0 = 10.20$, one calculates that with 60 phr ($\Phi_{black} = 0.213$), $\frac{T(\omega_1)}{\gamma}$ should be equal to 25.56, while the experimental result is nearly twice this value. The Guth–Gold equation is, however, based on mere hydrodynamic considerations and neither the complex structure of the filler nor the rubber–filler interactions are taken into consideration. Another interesting aspect is the growing difference between runs 1 and 2, as carbon black content in-

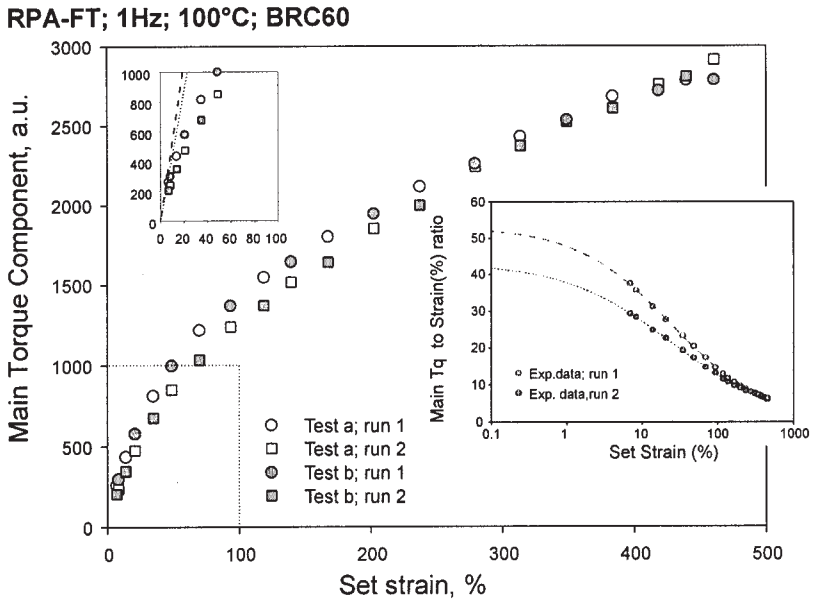

Figure 7 Main torque component when testing a 60-phr N330 filled BR compound (BRC60); deriving the modulus that would correspond to the linear response of the material.

creases. The first strain sequence softens the material and the higher the filler level the larger the strain softening effect. The parameter A in Eq. (2) is the reverse of a critical strain for the limit between the linear and the nonlinear behavior. As shown in the lower left plot in Figure 8, the higher the filler level, the lower this limit with no significant strain history effect. The lower right plot shows that the strain sensitivity parameter B steadily decreases with Φ_{black} and that mixing and compounding sig-

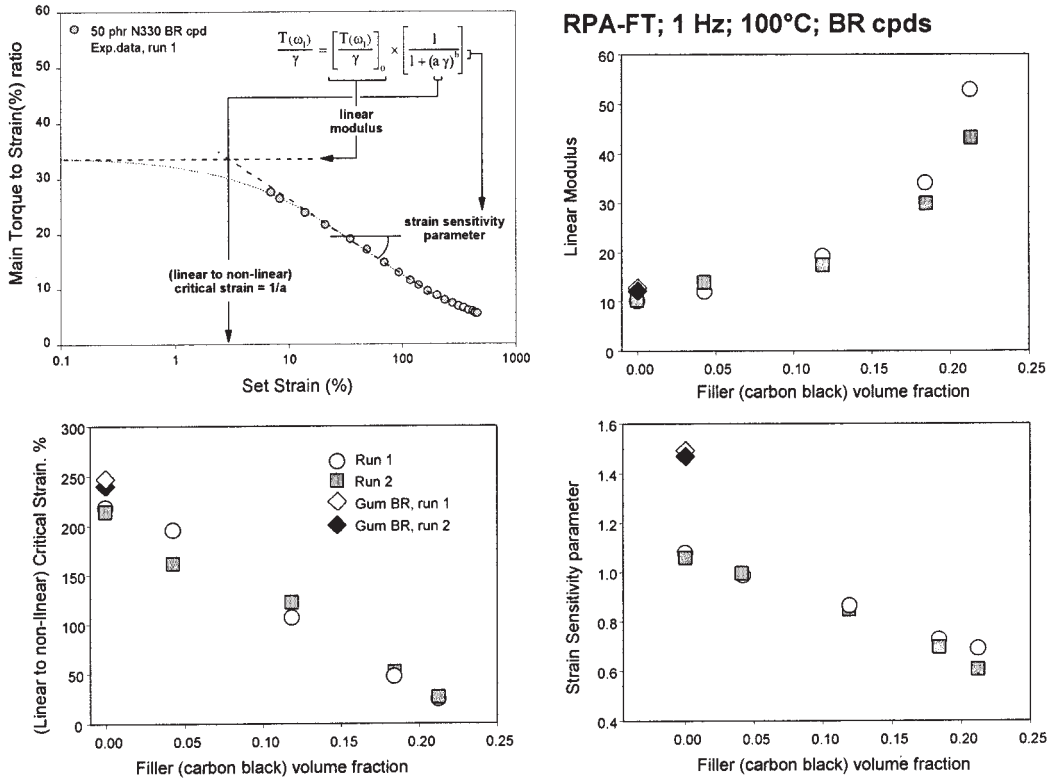

Figure 8 Effect of filler loading on parameters of Eq. (2), used to model the variation of modulus $T(\omega_1)/\gamma$ with strain.

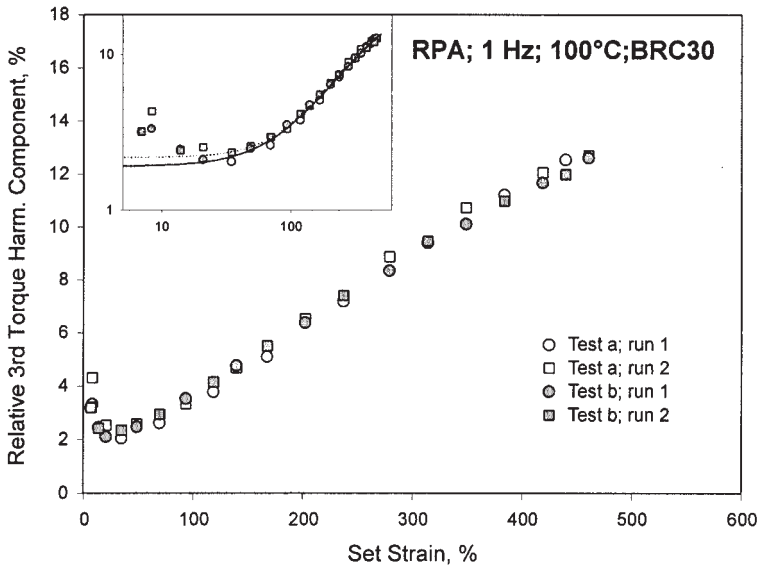

Figure 9 Relative third torque harmonic versus strain for the 30-phr carbon black filled polybutadiene compound (BRC30); two samples tested.

nificantly modify it (compare the gum BRN40 with the no-black compound BRC00).

Torque harmonics analysis

Through Fourier transform on 8192 (2^{13}) data points, harmonics up to $T(15\omega_1)$ or higher are detected but, above the fifth one, they become too small to be unambiguously distinguished from the noise. The limit of the relative torque harmonic $T(n\omega_1)/T(\omega_1)$[or $T(n/1)$] is expected to be equal to $1/n$, and $T(3/1)$ is consequently the most intense contribution compared to all other harmonics. The relative 3rd torque harmonic component is therefore the most interesting data for nonlinear viscoelastic characterization. All $T(3/1)$ data [and the corresponding $S(3/1)$] are given in Appendixes III and IV.

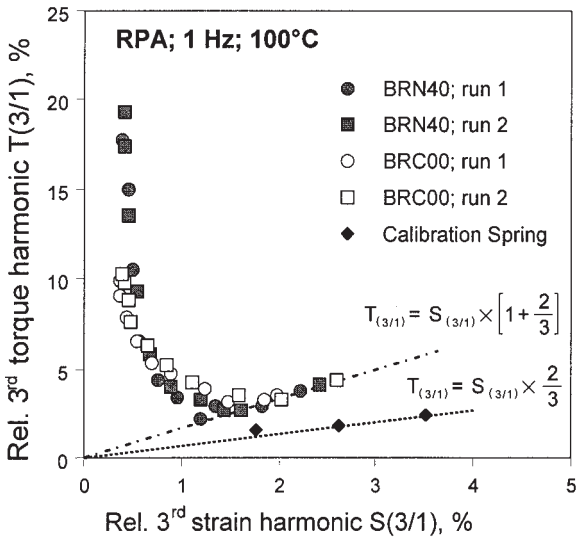

Figure 10 Relative third torque harmonic component $T(3/1)$ versus relative third strain harmonic component $S(3/1)$; BRN40 is gum polybutadiene and BRC00 is the zero black compound; for comparison, data obtained with a calibration spring are included.

As described in a previous publication[2], whatever the tested material, the variation of the relative 3rd torque harmonic component with the strain amplitude appears such that an *S*-shape curve is generally observed, from a (scattered) plateau value at low strain up to a maximum at high strain. Figure 9 shows this behavior in the case of the 30-phr filled compound. As can be seen, no significant strain history effect is detected since data for runs 1 and 2 superimpose well, and the material is well homogeneous (no difference between tests a and b). At low strain, data are scattered and $T(3/1)$ seems to locally decrease with increasing strain; such an effect has no physical sense and is in fact due to the deteriorating quality of the strain signal as the deformation angle decreases, as discussed above.

The simultaneous treatment of torque and strain signals through Fourier transform give access to both $T(n/1)$ and $S(n/1)$, which suggests that we should consider how the former is related to the latter, based on the obvious argument that the quality of the torque signal cannot be better than the one of the strain signal. Figure 10 shows plots of $T(3/1)$ versus $S(3/1)$ in the case of the gum polybutadiene (BRN40) and the zero black compound (BRC00).

To easily read Figure 10, one must keep in mind that the 3rd relative strain harmonic component $S(3/1)$ is

decreasing with increasing strain angle. Consequently, the large $T(3/1)$ values on the left of the graph correspond to the high strain region, and the small increase of $T(3/1)$ with higher $S(3/1)$ in the lower right part likely reflects the deteriorating quality of the strain signal in the low strain region. A few experiments were run with a calibration spring between the upper and lower dies.[17] In such a case, any harmonic in the strain signal is directly transmitted in the torque signal. As can be seen, $T(3/1)$ versus $S(3/1)$ data obtained with the calibration spring (i.e., as if a perfect elastic body was tested) fall on a straight line, which passes through zero and has a slope of 2/3. At this point, one could suspect that certain choices made by Alpha Technologies in developing the electronics of the instrument might be responsible for what appears to be an implicit defect in the strain signal; for instance, if the actual displacement of the RPA motor were coded in 24 bits and the strain signal be coded in 16 bits, then the origin of the $T(3/1)$ versus $S(3/1)$ slope in the case of a purely elastic body would be found ($16/24 = 2/3$). When the cavity is loaded, the torque signal measurement is made under pressurized conditions and we have shown in a previous section that the stiffness of the tested material does affect the quality of the strain signal, as considered through $S(3/1)$ [see Fig. 4]. Figure 10 shows that, either with the gum or with the compounded polybutadiene, the $T(3/1)$ versus $S(3/1)$ data in the low strain region are limited by a straight line, also passing through zero but with a different slope (in fact close to 5/3).

In fact, this simple picture, that a straight line of slope (A + 1/3) [with the actual value of A depending on the stiffness of the tested material] is marking the limit for $T(3/1)$ data reflecting essentially the nonlinear response of the material is not fully supported by results obtained when testing compounds with higher filler contents. Indeed, as shown in Figure 11, the low strain $T(3/1)$ versus $S(3/1)$ data for the filled materials seem to be limited by a straight line which has a slope between 2/3 and 5/3, with, however, a significant scatter occurring on data below the 5/3 slope limit. Obviously, the higher the stiffness of the material, the larger the nonlinear contribution of the latter in the measured torque response, with the immediate result that the instrument nonlinearity is overcome at a lower strain angle, as readily seen when comparing the $T(3/1)$ versus $S(3/1)$ plots for the 50- and 60-phr filled compounds (upper and lower parts of Fig. 11). The important aspect of Figure 11 is that one has now a unambiguous criterion to exclude $T(3/1)$ data that do not mainly express the nonlinearity of the material itself, independent of the instrument's nonlinearity in the low strain region. Accordingly, in studying how $T(3/1)$ is varying with strain γ, data will be systematically discarded when meeting the following criterion:

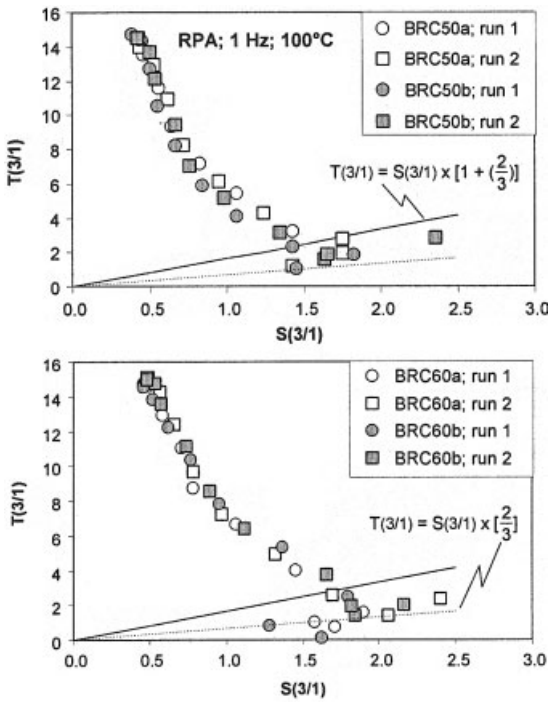

Figure 11 Relativethird torque harmonic component $T(3/1)$ versus relative third strain harmonic component $S(3/1)$ with highly filled polybutadiene compound; BRC50 is the 50-phr N330 compound and BRC60 is the 60-phr one; straight lines correspond to the $T(3/1)$ versus $S(3/1)$ linear relationship in the low strain region, either with the calibration spring (slope 2/3) or with the gum BR (slope 5/3).

$$\frac{T(3/1) - S(3/1)}{S(3/1)} < 0.67.$$

The typical S-shape variation of $T(3/1)$ on strain was shown in Figure 9 in the case of the 30-phr carbon black compound (BRC30). Similar plots were obtained with the other test materials, with, however, some differences imparted to the filler level. In a previous publication,[18] a simple equation was used to model the observed $T(3/1)$ behavior, from a limiting plateau value at low strain, i.e., $T(3/1)_{min}$, toward a maximum plateau value at high (infinite) strain, i.e., $T(3/1)_{max}$, according to

$$T(3/1)_\gamma = T(3/1)_{min} + [T(3/1)_{max} - T(3/1)_{min}] \times [1 - \exp(-C\gamma)]^D, \quad (3)$$

where γ is the deformation (%), and C and D are fit parameters.[3] Figure 12 illustrates how the model fits well the measured data in the nonlinear region of interest, i.e., when strain is larger than 50%. The inset is a magnification of the low strain region through logarithmic scaling; the brackets indicate data that were not considered for the nonlinear fitting of Eq. (3), with respect to the discarding rule

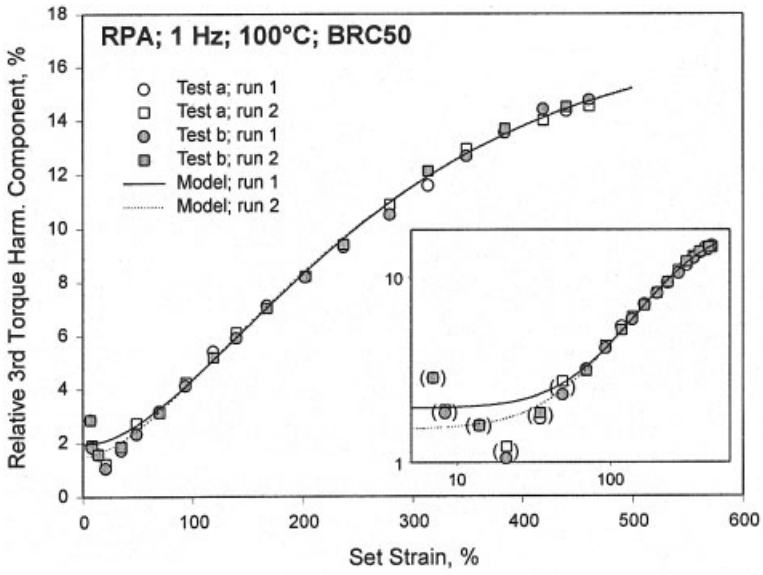

Figure 12 Modeling the strain dependence of the third relative torque harmonic by means of Eq. (3), in the case of a 50-phr carbon black filled BR compound (BRC50); the inset is a magnification of the low strain region through logarithmic scaling; brackets indicate data that were not used in nonlinear fitting.

described above. Except in the low strain region, where torque signal nonlinearity is essentially reflecting instrument's limitation, data and fitting appear very reproducible with no difference between tests a and b and no difference between runs 1 and 2. This proves that the tested compound does not exhibit any strain history effect, or in other terms, that rubber–filler interactions resist large strain amplitude (i.e., up to 500% at 1 Hz).

Table IV gives the fit parameters of Eq. (3) for all the materials tested. Correlation coefficients are excellent (>0.98) and except for test BRC00, tests a and b lead to similar parameter values. The values of the limiting harmonics $T(3/1)_{min}$ and $T(3/1)_{max}$ have relatively little meaning in the experimental context, the former for the reasons explained above and the latter because the maximum permitted strain (33°, or 461%) at 1 Hz gives access to experimental data that are quite far from the plateau at infinite strain. When considering $T(3/1)$ versus γ plots with the highly filled materials (see Fig. 12, for instance), there is no doubt, however, that the $T(3/1)_{max}$ plateau exists, and it has been clearly seen elsewhere when testing other materials, either gum EPDMs[2] or gum SBRs[15]. Data in Table IV tend to show that $T(3/1)_{max}$ decreases with higher filled loading. With respect to nonlinear viscoelastic behavior, the most significant information is, however, provided by the two parameters C and D that "quantify" the strain sensitivity of materials. Analyzing strain sensitivity through two parameters, which are somehow dependent on each other, is nevertheless complicated

TABLE IV
Modeling the Variation of the Third Relative Torque Harmonic with Strain; Fit Parameters of Eq. (3)

Model:	$T(3/1)_\gamma = T(3/1)_{min} + [T(3/1)_{max} - T(3/1)_{min}]\times[1 - \exp(-C_\gamma)]^D$				
Test	$T(3/1)_{min}$	$T(3/1)_{max}$	C	D	r^2
BRN40, run 1	2.62	39.32	3.65×10^{-3}	3.90	0.9983
BRN40, run 2	2.73	31.84	4.60×10^{-3}	4.37	0.9988
BRC00, run 1	3.01	29.33	9.90×10^{-4}	1.28	0.9963
BRC00, run 2	3.60	12.45	4.96×10^{-3}	2.70	0.9909
BRC10, run 1	3.84	20.42	2.49×10^{-3}	2.02	0.9806
BRC10, run 2	3.80	14.18	4.46×10^{-3}	2.09	0.9905
BRC30, run 1	1.91	21.05	2.80×10^{-3}	1.76	0.9980
BRC30, run 2	2.18	16.64	4.30×10^{-3}	2.22	0.9985
BRC50, run 1	1.95	17.35	5.34×10^{-3}	2.10	0.9984
BRC50, run 2	1.50	17.62	4.98×10^{-3}	1.85	0.9984
BRC60, run 1	0.97	16.13	6.42×10^{-3}	1.56	0.9971
BRC60, run 2	2.33	16.40	7.55×10^{-3}	2.49	0.9978

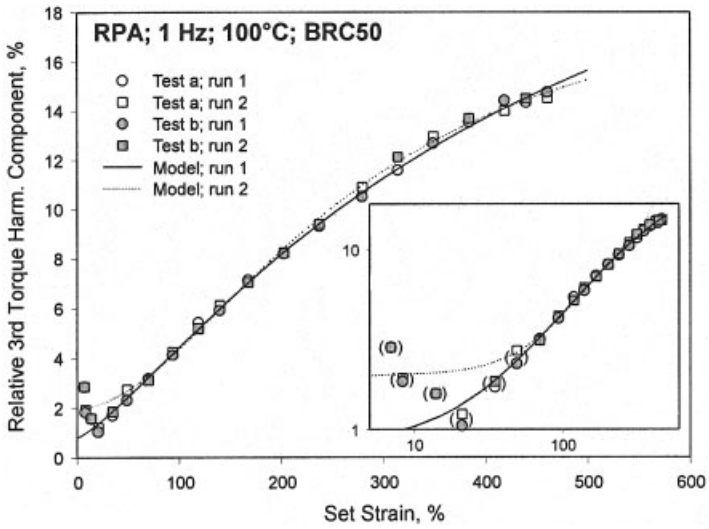

Figure 13 Modeling the strain dependence of the third relative torque harmonic by means of Eq. (5), in the case of a 50-phr carbon black filled BR compound (BRC50); the inset is a magnification of the low strain region through logarithmic scaling; brackets indicate data that were not used in nonlinear fitting.

but, as we shall see below, there is an easy manner to circumvent this difficulty.

In his important contribution to Fourier transform rheometry, Wilhelm[11] observed also significant variations of the 3rd harmonic torque component and proposed the following model (rewritten using our formalism):

$$T(3/1) = B \times \left[1 - \frac{1}{1 + (c\gamma)^d}\right], \qquad (4)$$

where B is the maximum possible third harmonic contribution at idealized infinite shear amplitude, c is a critical inverse strain amplitude, and d is a parameter describing the strain sensitivity. One notes that if $\gamma = \frac{1}{c}$, then $T(3/1) = \frac{B}{2}$, and that Eq. (4) explicitly considers that $T(3/1) = 0$ at zero strain. However, when performing very low shear experiments on various polymer systems, Wilhelm et al.[6] observed that, even for very small strain amplitudes, nonlinear contributions could still be detected via the third harmonic contributions, which they attributed to instrumentation limits in the very low shear region. Indeed from a theoretical point of view, the linear viscoelastic regime would be by definition characterized by the absence of harmonics in the torque signal. We tend to share the same point of view, which calls obviously for further instrumental development in accurately investigating the very low strain region.

Our interest in Fourier transform rheometry, however, is essentially in the capability this technique offers to investigate the nonlinear viscoelastic region and particularly the strain sensitivity of polymer materials. Consequently, with respect to our model that explicitly considers a limiting $T(3/1)_{\min}$ in the low shear region, the Wilhelm model was slightly modified to consider a non-zero low strain torque harmonic, i.e.,

$$T(3/1)_\gamma = T(3/1)_{\min} + [T(3/1)_{\max} - T(3/1)_{min}] \times \left[1 - \frac{1}{1 + (c\gamma)^d}\right]. \qquad (5)$$

Figure 13 shows how this model fit the data of the 50-phr compound; all fit parameters for the materials investigated are given in Table V. There are some (minor) differences in the manner in which Eqs. (3) and (5) are meeting the measured data, but the fit quality is essentially the same ($r^2 > 0.98$).

It is worth emphasizing here an important aspect of nonlinear fitting. Most available fitters are based on the Marquardt–Levenberg algorithm, which seeks the values of the parameters that minimize the sum of the squared differences between the values of the observed (i.e., experimental data) and predicted values of the dependent variable. The Marquardt–Levenberg process is iterative and therefore the curve fitter begins with a "guess" at the parameters. In our calculations, we used ML algorithms available either in MathCad 8 (MathSoft, Inc.) or in SigmaPlot 8.0 (SPSS Software); essentially identical results are obtained with both software packages, providing that adequate initial guesses are considered. In fitting either Eq. (3) or (5), we used systematically the guesses

initial value for $T(3/1)_{\min}$ = lowest $T(3/1)$ value;

TABLE V
Modeling the Variation of the Third Relative Torque Harmonic with Strain; Fit Parameters of Eq. (5)

Model: $T(3/1)_\gamma = T(3/1)_{min} + [T(3/1)_{max} - T(3/1)_{min}] \times \left[1 - \frac{1}{1 + (c\,\gamma)^d}\right]$					
Test	$T(3/1)_{min}$	$T(3/1)_{max}$	c	d	r^2
BRN40, run 1	2.58	35.21	2.18×10^{-3}	2.84	0.9985
BRN40, run 2	2.69	30.64	2.47×10^{-3}	2.93	0.9991
BRC00, run 1	3.01	38.91	7.30×10^{-4}	1.26	0.9964
BRC00, run 1	3.57	13.53	3.01×10^{-3}	2.11	0.9905
BRC10, run 1	3.82	23.36	1.70×10^{-3}	1.77	0.9805
BRC10, run 2	3.77	16.06	2.98×10^{-3}	1.79	0.9904
BRC30, run 1	1.87	25.62	1.95×10^{-3}	1.60	0.9980
BRC30, run 2	2.14	18.98	2.83×10^{-3}	1.87	0.9985
BRC50, run 1	0.81	28.26	2.27×10^{-3}	1.27	0.9984
BRC50, run 2	1.98	19.61	3.66×10^{-3}	1.85	0.9982
BRC60, run 1	1.63	17.76	5.33×10^{-3}	1.74	0.9968
BRC60, run 2	2.46	17.68	4.90×10^{-3}	2.12	0.9973

initial value for $[T(3/1)_{max} - T(3/1)_{min}]$ = highest $T(3/1)$ value;

initial guessed C(or c)= $T(3/1)|_{250\%}$;

initial guessed D(or d)= $\frac{dT(3/1)}{d\gamma}|_{250\%}$.

Satisfactory convergence was generally obtained within 100 iterations. Fit parameters were rounded to significant decimals and fit curves were calculated with rounded parameters (as given in Tables IV and V)

$T(3/1)_{min}$ and $T(3/1)_{max}$ values, as obtained through the use of Eq. (5), may receive the same comments as for Eq. (3), and one would hardly be more confident in the values obtained using the former or the latter equation. Parameters c,C and d,D, while having values in similar ranges for both equations, have obviously different mathematical virtues. Whatever the equation, however, one must consider both c,C and d,D to assess the strain sensitivity of the tested materials, quite a complicated manner to compare different material responses.

An elegant manner to overcome this difficulty consists of considering the first derivatives of the above equation to calculate the slope of $T(3/1)$ versus γ curves at any strain. Such derivatives are, respectively,

$$S1(\gamma) = \frac{dT(3/1)}{d\gamma} = [T(3/1)_{max} - T(3/1)_{min}] \times C \times D \times \exp(-C\gamma) \times [1 - \exp(-C\gamma)^{D-1} \quad (6)$$

and

$$S2(\gamma) = \frac{dT(3/1)}{d\gamma} = \frac{[T(3/1)_{max} - T(3/1)_{min}] \times d \times (-c\gamma)^d}{\gamma \times [1 + (c\gamma)^d]^2}. \quad (7)$$

Slopes at $\gamma = 250\%$ as well as $T(3/1)$ at the same strain were calculated using Eqs. (6) and (7) with the corresponding values of C, c and D, d. Results, given in Table VI, show that both models give similar results. Slopes $S1$ (250%) and $S2$ (250%) reflect the strain sensitivity of materials at 250% and offer a direct, nonambiguous quantification of their nonlinear viscoelastic character and an easy manner to assess the effects of compounding differences, as illustrated in Figure 14.

As expected, $T(3/1)$ at 250% strain and $\frac{dT(3/1)}{d\gamma}$ at $\gamma = 250\%$ (as calculated with Eqs. (3) and (6)) vary with filler volume fraction. The relative third harmonic torque component $T(3/1)_{250}$ is, however, not much affected by filler loading up to $\phi_{black} \approx 0.13$ (corresponding to 30 phr); then a significant increase is observed for higher filler fractions. No significant difference on $T(3/1)_{250}$ is seen between the gum and the zero black compound. The information provided by this parameter is in fact very similar to that observed with the linear modulus (compare with Fig. 8, upper right graph). The slope $\frac{dT(3/1)}{d\gamma}|_{250\%}$ offers a different picture of nonlinear viscoelasticity. As can be seen in the lower part of Figure 14, a there is significant difference between the gum and the zero black compound, with the latter less sensitive to strain. The nonlinear character (slightly) increases with ϕ_{black} until the critical volume fraction of 0.13 is reached; above this filler loading, strain sensitivity begins to decrease and, because differences are observed between results from runs 1 and 2, strain history appears then to play a role. In other terms, above $\phi_{black} \approx 0.13$, straining a filled compound up to 500% (in harmonic conditions) either produces permanent damage in the rubber–filler morphology or produce changes that need more than 2 min resting time to be recovered.

TABLE VI
Assessing Strain Sensitivity through Slope of *T*(3/1) versus Strain Curves

	Eqs. (3) and (6)		Eqs. (5) and (7)	
Model :	$T(3/1)$ at $\gamma = 250\%$	$\frac{dT(3/1)}{d\gamma}$ at $\gamma = 250\%$	$T(3/1)$ at $\gamma = 250\%$	$\frac{dT(3/1)}{d\gamma}$ at $\gamma = 250\%$
BRN40, run 1	7.57	0.0473	7.52	0.0476
BRN40, run 2	8.25	0.0514	8.16	0.0516
BRC00, run 1	6.79	0.0170	6.78	0.0170
BRC00, run 2	7.11	0.0192	7.10	0.0192
BRC10, run 1	7.35	0.0204	7.34	0.0204
BRC10, run 2	8.33	0.0206	8.33	0.0205
BRC30, run 1	7.63	0.0278	7.58	0.0278
BRC30, run 2	7.90	0.0283	7.93	0.0284
BRC50, run 1	10.06	0.0325	9.80	0.0307
BRC50, run 2	10.10	0.0320	10.08	0.0324
BRC60, run 1	11.66	0.0269	11.67	0.0264
BRC60, run 2	11.68	0.0314	11.68	0.0308

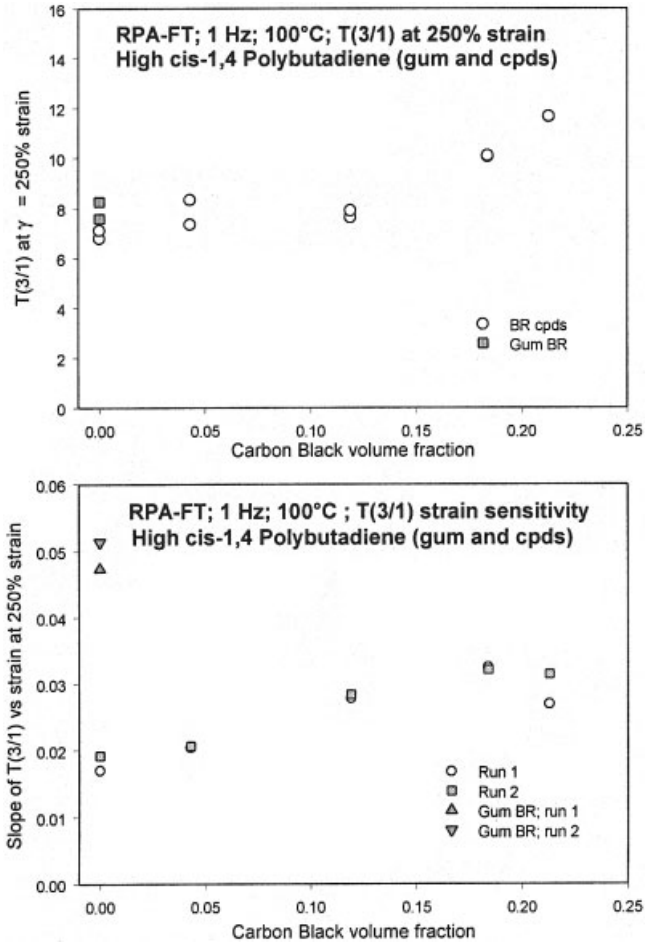

Figure 14 Effect of filler loading on nonlinear viscoelastic parameters as obtained through Fourier transform rheometry; $\frac{dT(3/1)}{d\gamma}$ and $\frac{T(3/1)}{d\gamma}\Big|_{250\%}$ were calculated with Eqs. (3) and (6), respectively, and parameters given in Table IV.

CONCLUSIONS

The nonlinear viscoelastic behavior of carbon black filled polybutadiene compounds is conveniently investigated through Fourier transform rheometry, as performed with a modified Rubber Process Analyzer. Strain sweep test protocols prove to be methods of choice in gaining reproducible results, particularly in the high strain region, thanks to the closed test cavity design of the instrument.

Fourier transform spectra contain all the information available through harmonic testing, without any condition, as is the case with linear dynamic testing, which requires insensitivity of the modulus on strain amplitude. In addition, FT rheometry is very accurate since one can easily distinguish the main torque component (i.e., the first harmonic at the test frequency) from other harmonics whose relative intensity significantly increases with strain amplitude.

A testing procedure, involving two subsequent strain sweep tests and applied to two samples of test material, shows that strain history effects occur only when the filler fraction is larger than 12–13%. Below this level, the nonlinear response of compounds is mainly due to the rubber matrix, with the filler particles playing essentially a hydrodynamic role.

Differences in nonlinear behavior, due to growing filler level, are easily and clearly detected and the dependence upon strain of the relative third harmonic component is adequately modeled with simple four-parameter models. Two such models were compared and found to give similar results, both offering two parameters to describe the strain sensitivity. First derivatives of the models allow a single number, i.e., the slope at a given strain, to be calculated as a "quantification" of the strain sensitivity, and hence of the nonlinear character. Carbon

black volume fraction appears then as the main compounding parameter influencing the nonlinear viscoelastic response.

The work reported shows clearly some of the instrument's limits, particularly in the low strain region, where the quality of the applied strain signal deteriorates as the strain amplitude decreases. Harmonics occurs in the strain signals below 50% strain that may reflect some intrinsic deficiencies in the manner in which the electronic system is operated. However, as the strain amplitude decreases, the response of the tested materials is expected to be essentially linear and consequently only the main component is of importance. The knowledge of instrument's limitation is important for nonlinear testing as a simple criterion is derived for sorting out valid (harmonic) data that reflect essentially the nonlinear response of test materials.

TABLE A.I
RPA - FT (1 Hz; 100°C) Main Signal Components (a.u.); Fourier Transform on 8192 Data Points at 512 pt/s (16 cycles)

Sample code: Test:		BRC00 Test a Run 1		BRC10 Test a Run 1		BRC30 Test a Run 1		BRC50 Test a Run 1		BRC60 Test a Run 1		BRN40 Test a Run 1	
Strain (%)	Strain (deg)	Torque	Strain	Torque	Strain	Torque	Strain	Torque	Strain	Torque	Strain	Torque	Strain
6.98	0.50	68.97	22.57	80.51	22.58	123.90	22.39	192.90	22.56	261.80	22.53	83.55	22.55
13.96	1.00	135.10	45.32	156.90	45.31	228.70	45.33	333.20	45.31	436.10	45.29	166.50	45.47
34.91	2.50	314.50	113.80	365.50	113.70	494.40	113.90	665.80	114.00	815.10	113.80	405.50	113.80
69.81	5.00	551.80	227.70	632.40	227.50	816.80	227.80	1030.00	227.70	1220.00	227.80	743.60	227.70
118.68	8.50	792.40	387.00	902.70	387.00	1109.00	387.00	1364.00	386.90	1550.00	387.00	1079.00	387.10
167.55	12.00	965.70	546.40	1094.00	546.40	1314.00	546.50	1605.00	546.70	1804.00	546.50	1300.00	546.60
237.36	17.00	1141.00	774.20	1288.00	774.10	1540.00	773.90	1880.00	774.00	2119.00	774.20	1485.00	774.30
314.16	22.50	1283.00	1025.00	1463.00	1025.00	1729.00	1025.00	2141.00	1025.00	2428.00	1024.00	1578.00	1025.00
383.97	27.50	1391.00	1253.00	1605.00	1252.00	1867.00	1253.00	2338.00	1252.00	2684.00	1252.00	1611.00	1252.00
439.82	31.50	1467.00	1435.00	1703.00	1435.00	1971.00	1435.00	2455.00	1435.00	2787.00	1435.00	1643.00	1435.00
Strain	Strain	Run 2		Run 2		Run 2		Run 2		Run 2		Run 2	
(%)	(deg)	Torque	Strain	Torque	Strain	Torque	Strain	Torque	Strain	Torque	Strain	Torque	Strain
8.38	0.60	83.62	27.13	139.50	34.72	133.70	27.14	194.90	27.17	238.20	27.15	103.20	27.34
20.94	1.50	198.40	68.07	260.90	68.10	299.20	68.03	408.00	68.08	474.50	68.07	252.80	68.04
48.87	3.50	417.80	159.40	532.30	159.20	595.30	159.50	753.80	159.50	849.40	159.50	561.70	159.80
93.55	6.70	681.30	304.90	830.70	304.90	919.30	304.90	1118.00	304.80	1238.00	304.80	935.50	304.80
139.63	10.00	874.20	455.40	1041.00	455.20	1154.00	455.20	1390.00	455.40	1516.00	455.50	1196.00	455.60
202.46	14.50	1059.00	660.40	1243.00	660.40	1396.00	660.20	1686.00	660.30	1852.00	660.40	1412.00	660.50
279.25	20.00	1217.00	910.60	1430.00	911.10	1618.00	910.60	1995.00	910.80	2254.00	911.00	1541.00	911.10
349.07	25.00	1335.00	1139.00	1567.00	1139.00	1782.00	1139.00	2225.00	1139.00	2523.00	1139.00	1595.00	1139.00
418.88	30.00	1438.00	1366.00	1672.00	1367.00	1917.00	1367.00	2403.00	1366.00	2758.00	1366.00	1626.00	1367.00
460.77	33.00	1489.00	1503.00	1718.00	1504.00	1980.00	1503.00	2487.00	1503.00	2913.00	1503.00	1646.00	1503.00

TABLE A.II
RPA - FT (1 Hz; 100°C) Main Signal Components (a.u.); Fourier Transform on 8192 Data Points at 512 pt/s (16 cycles)

Sample code: Test:		BRC00 Test b Run 1		BRC10 Test b Run 1		BRC30 Test b Run 1		BRC50 Test b Run 1		BRC60 Test b Run 1		BRN40 Test b Run 1	
Strain (%)	Strain (deg)	Torque	Strain	Torque	Strain	Torque	Strain	Torque	Strain	Torque	Strain	Torque	Strain
8.38	0.60	82.05	27.11	95.94	27.07	145.00	27.11	221.40	27.15	299.60	27.13	100.80	27.28
20.94	1.50	196.50	68.03	226.90	67.99	317.70	68.06	454.60	68.04	580.00	68.05	248.00	68.08
48.87	3.50	415.50	159.50	467.60	159.30	621.50	159.50	838.60	159.50	999.80	159.60	554.30	159.90
93.55	6.70	676.10	304.90	744.50	305.10	940.00	304.80	1210.00	304.90	1373.00	304.90	926.70	304.90
139.63	10.00	867.00	455.40	949.70	455.20	1172.00	455.30	1485.00	455.20	1646.00	455.30	1189.00	455.50
202.46	14.50	1055.00	660.50	1154.00	660.30	1400.00	660.20	1775.00	660.30	1947.00	660.50	1410.00	660.40
279.25	20.00	1216.00	910.60	1347.00	910.60	1617.00	910.70	2052.00	910.70	2256.00	910.90	1537.00	911.10
349.07	25.00	1329.00	1138.00	1499.00	1139.00	1773.00	1138.00	2279.00	1139.00	2538.00	1139.00	1590.00	1139.00
418.88	30.00	1434.00	1367.00	1631.00	1366.00	1907.00	1367.00	2458.00	1367.00	2720.00	1366.00	1633.00	1367.00
460.77	33.00	1490.00	1503.00	1710.00	1503.00	1982.00	1503.00	2531.00	1503.00	2788.00	1503.00	1654.00	1503.00
		Run 2		Run 2		Run 2		Run 2		Run 2		Run 2	
Strain (%)	Strain (deg)	Torque	Strain	Torque	Strain	Torque	Strain	Torque	Strain	Torque	Strain	Torque	Strain
6.98	0.50	69.05	22.59	92.77	22.60	123.90	22.39	169.40	22.56	205.20	22.56	86.64	22.75
13.96	1.00	133.90	45.32	179.00	45.33	208.90	45.34	296.70	45.31	347.90	45.28	171.20	45.49
34.91	2.50	310.50	113.80	405.40	113.70	451.90	114.00	609.00	113.90	677.00	113.90	415.80	113.90
69.81	5.00	548.70	227.70	681.80	227.40	748.40	227.60	959.60	227.80	1034.00	227.60	758.90	227.80
118.68	8.50	789.20	386.80	943.70	386.90	1037.00	386.70	1284.00	387.00	1372.00	386.90	1096.00	387.10
167.55	12.00	959.00	546.50	1125.00	546.30	1247.00	546.50	1541.00	546.40	1642.00	546.50	1311.00	546.50
237.36	17.00	1129.00	774.00	1319.00	774.40	1484.00	773.80	1845.00	774.10	1999.00	773.90	1481.00	774.40
314.16	22.50	1270.00	1025.00	1489.00	1025.00	1687.00	1024.00	2139.00	1024.00	2369.00	1024.00	1563.00	1025.00
383.97	27.50	1386.00	1252.00	1610.00	1253.00	1832.00	1252.00	2373.00	1252.00	2609.00	1252.00	1610.00	1253.00
439.82	31.50	1463.00	1434.00	1685.00	1435.00	1926.00	1435.00	2483.00	1434.00	2809.00	1435.00	1646.00	1435.00

TABLE A.III
RPA - FT (1 Hz; 100°C) Relative Third Harmonic Components; Fourier Transform on 8192 Data Points at 512 pt/s (16 cycles)

Sample code: Test:		BRC00 Test a Run 1		BRC10 Test a Run 1		BRC30 Test a Run 1		BRC50 Test a Run 1		BRC60 Test a Run 1		BRN40 Test a Run 1	
Strain (%)	Strain (deg)	*T*(3/1), %	*S*(3/1), %	*T*(3/1), %	*S*(3/1), %	*T*(3/1), %	*S*(3/1), %	*T*(3/1), %	*S*(3/1), %	*T*(3/1), %	*S*(3/1), %	*T*(3/1), %	*S*(3/1), %
6.98	0.50	3.25	1.85	5.35	3.41	3.19	2.11	2.85	2.36	1.01	1.57	3.78	2.23
13.96	1.00	3.45	1.99	3.74	2.22	2.45	1.80	1.58	1.64	0.77	1.71	2.90	1.84
34.91	2.50	3.19	1.49	2.90	1.43	2.05	1.41	1.72	1.64	1.63	1.90	2.18	1.21
69.81	5.00	3.89	1.25	3.96	1.06	2.62	1.21	3.18	1.43	4.05	1.45	2.85	1.35
118.68	8.50	4.65	0.90	4.82	0.67	3.79	0.80	5.42	1.07	6.65	1.06	3.36	0.96
167.55	12.00	5.37	0.69	5.73	0.43	5.10	0.58	7.15	0.82	8.76	0.78	4.35	0.76
237.36	17.00	6.51	0.54	7.13	0.35	7.19	0.46	9.32	0.64	11.05	0.71	6.56	0.58
314.16	22.50	7.90	0.44	8.67	0.30	9.40	0.37	11.59	0.56	12.96	0.58	10.53	0.51
383.97	27.50	9.08	0.37	10.25	0.28	11.22	0.32	13.54	0.46	14.59	0.49	14.94	0.45
439.82	31.50	9.92	0.36	11.31	0.30	12.55	0.31	14.35	0.46	14.77	0.46	17.77	0.40
		Run 2		Run 2		Run 2		Run 2		Run 2		Run 2	
Strain (%)	Strain (deg)	*T*(3/1), %	*S*(3/1), %	*T*(3/1), %	*S*(3/1), %	*T*(3/1), %	*S*(3/1), %	*T*(3/1), %	*S*(3/1), %	*T*(3/1), %	*S*(3/1), %	*T*(3/1), %	*S*(3/1), %
8.38	0.60	4.30	2.60	5.44	3.73	4.31	2.78	1.91	1.75	2.35	2.40	4.14	2.42
20.94	1.50	3.24	2.02	3.69	2.07	2.53	1.68	1.21	1.43	1.38	2.06	2.67	1.63
48.87	3.50	3.47	1.58	3.76	1.25	2.57	1.29	2.73	1.75	2.56	1.69	2.71	1.43
93.55	6.70	4.26	1.11	4.92	0.79	3.33	0.92	4.26	1.24	4.92	1.32	3.22	1.19
139.63	10.00	5.14	0.85	6.00	0.57	4.68	0.72	6.12	0.95	7.20	0.97	4.00	0.89
202.46	14.50	6.25	0.65	7.40	0.48	6.52	0.54	8.24	0.71	9.70	0.78	5.78	0.68
279.25	20.00	7.61	0.47	8.83	0.37	8.87	0.45	10.89	0.62	12.38	0.66	9.35	0.55
349.07	25.00	8.79	0.46	10.07	0.33	10.73	0.35	12.94	0.53	14.23	0.57	13.56	0.46
418.88	30.00	9.77	0.40	11.16	0.27	12.06	0.31	14.00	0.44	15.11	0.49	17.43	0.43
460.77	33.00	10.25	0.39	11.84	0.28	12.71	0.27	14.52	0.43	15.08	0.48	19.29	0.41

TABLE A.IV
RPA - FT (1 Hz; 100°C) Relative Third Harmonic Components; Fourier Transform on 8192 Data Points at 512 pt/s (16 cycles)

Sample code: Test:		BRC00 Test b Run 1		BRC10 Test b Run 1		BRC30 Test b Run 1		BRC50 Test b Run 1		BRC60 Test b Run 1		BRN40 Test b Run 1	
Strain (%)	Strain (deg)	$T(3/1)$, %	$S(3/1)$, %	$T(3/1)$, %	$S(3/1)$, %	$T(3/1)$, %	$S(3/1)$, %	$T(3/1)$, %	$S(3/1)$, %	$T(3/1)$, %	$S(3/1)$, %	$T(3/1)$, %	$S(3/1)$, %
8.38	0.60	2.61	1.54	6.65	4.14	3.33	2.25	1.84	1.83	0.84	1.29	3.21	1.71
20.94	1.50	3.32	1.99	4.95	2.94	2.11	1.54	1.05	1.46	0.16	1.62	1.49	0.78
48.87	3.50	3.59	1.62	4.17	1.55	2.48	1.34	2.32	1.43	2.48	1.79	2.55	1.33
93.55	6.70	4.29	1.15	4.69	0.77	3.53	1.00	4.13	1.06	5.34	1.37	3.23	1.24
139.63	10.00	4.85	0.79	5.48	0.54	4.77	0.75	5.92	0.85	7.85	0.96	3.91	0.90
202.46	14.50	5.90	0.61	6.55	0.41	6.39	0.52	8.21	0.67	10.36	0.77	5.49	0.70
279.25	20.00	7.25	0.45	7.84	0.31	8.35	0.43	10.52	0.55	12.26	0.62	9.16	0.55
349.07	25.00	8.53	0.34	9.21	0.29	10.12	0.41	12.68	0.51	13.85	0.52	13.20	0.49
418.88	30.00	9.63	0.32	10.66	0.28	11.68	0.35	14.42	0.44	14.65	0.47	16.86	0.46
460.77	33.00	10.24	0.30	11.48	0.30	12.62	0.33	14.76	0.39	14.55	0.46	18.97	0.45
		Run 2		Run 2		Run 2		Run 2		Run 2		Run 2	
Strain (%)	Strain (deg)	$T(3/1)$, %	$S(3/1)$, %	$T(3/1)$, %	$S(3/1)$, %	$T(3/1)$, %	$S(3/1)$, %	$T(3/1)$, %	$S(3/1)$, %	$T(3/1)$, %	$S(3/1)$, %	$T(3/1)$, %	$S(3/1)$, %
6.98	0.50	4.74	2.96	6.54	4.10	3.19	2.11	2.85	2.36	2.01	2.16	5.43	3.18
13.96	1.00	3.72	2.25	4.68	2.80	2.42	1.61	1.58	1.64	1.42	1.84	2.38	1.39
34.91	2.50	3.19	1.67	3.51	1.66	2.34	1.35	1.85	1.66	1.92	1.82	2.72	1.57
69.81	5.00	3.68	1.25	4.33	0.98	2.94	1.16	3.12	1.35	3.76	1.65	2.95	1.43
118.68	8.50	4.61	0.83	5.55	0.62	4.14	0.83	5.19	0.98	6.38	1.12	3.56	0.98
167.55	12.00	5.56	0.66	6.73	0.46	5.50	0.67	7.05	0.76	8.55	0.89	4.71	0.78
237.36	17.00	6.81	0.53	8.08	0.39	7.40	0.53	9.40	0.67	11.10	0.74	7.63	0.62
314.16	22.50	8.17	0.41	9.41	0.30	9.46	0.45	12.12	0.53	13.59	0.57	12.07	0.53
383.97	27.50	9.30	0.38	10.48	0.25	10.99	0.36	13.69	0.50	14.77	0.54	15.87	0.47
439.82	31.50	10.05	0.32	11.32	0.24	11.99	0.37	14.49	0.42	14.98	0.48	18.27	0.45

References

1. Leblanc, J. L.; de la Chapelle, C. Rubb Chem Technol 2003, 76, 287.
2. Leblanc, J. L. J Appl Polym Sci 2003, 89, 1101.
3. Payne, A. R.; Whittaker, R. E. Rubb Chem Technol 1971, 44, 440.
4. Wang, M. J. Rubb Chem Technol 1998, 71, 520.
5. Maier, P. G.; Göritz, D. Kautsch Gummi Kunstst 1996, 49, 18.
6. Chazeau, L.; Brown, J. D.; Yanyo, L. C.; Sternstein, S. S. Polym Compos 2000, 21, 202.
7. Sternstein, S. S.; Zhu, A. Macromolecules 2002, 35, 7262.
8. Leblanc, J. L. Kautsch Gummi Kunstst 1996, 49, 258
9. Leblanc, J. L. Prog Polym Sci 2002, 27, 627.
10. Leblanc, J. L.; Mongruel, A. Prog Rubb Plast Technol 2001, 17, 162.
11. Wilhelm, M. Macromol Mater Eng 2002, 287, 83.
12. Wilhelm, M.; Reinheimer, P.; Ortseifer, M. Rheol Acta 1999, 38, 349.
13. Guth, E.; Simha, R. Kolloid Zeitschrift 1936, 74, 266
14. Guth, R.; Gold, O. Phys Rev 1938, 53, 322.
15. Leblanc, J. L. Investigating the non-linear viscoelastic behaviour of rubber materials through Fourier transform rheometry, 9th International Seminar on Elastomers, Kyoto, Japan, April 3–5, 2003.
16. Note that in this paper, $I(n\omega_1)/I(\omega_1)$ or the abridged form $I(n/1)$, is used to describe the nth relative harmonic component of any harmonic signal; $S(n\omega_1)/S(\omega_1)$ or $S(n/1)$ specifically means that a strain signal is considered; $T(n\omega_1)/T(\omega_1)$ or $T(n/1)$ is used for the torque signal.
17. By courtesy of H. Buhrin (Alpha Technologies); strain and torque signals were acquired (10,240 pt at 512 pt/s) on another RPA instrument, equipped with a similar data acquisition system; FT was performed with our calculation algorithm using 8192 data points.
18. In using Eq. (3) (and subsequent ones) to model $T(3/1)$ variation with strain, one may express the deformation (or strain) γ either in degree angle or in percentages. Obviously, all parameters remain the same except C, whose value depends on the unit for γ. The following equality applies for the conversion, $C(\gamma, \text{deg}) = \frac{180\ \alpha}{100\ \pi} \times C(\gamma, \%)$, where $\alpha = 0.125$ rad.